

Active Pulleys: Magnetic Resonance Imaging of Rectus Muscle Paths in Tertiary Gazes

Reika Kono,^{1,2} Robert A. Clark,¹ and Joseph L. Demer^{1,3}

PURPOSE. The orbital layer of each rectus extraocular muscle (EOM) inserts on connective tissue, and the global layer inserts on the eyeball. The active-pulley hypothesis (APH) proposes that a condensation of this connective tissue constitutes a pulley serving as the functional origin of the rectus EOM, and that this pulley makes coordinated, gaze-related translations along the EOM axis to implement a linear ocular motor plant. This study was designed to measure gaze-related shifts in EOM pulley locations.

METHODS. Magnetic resonance imaging (MRI) was performed in eight normal volunteers in 2-mm thickness coronal planes perpendicular to the orbital axis for nine cardinal gaze directions. Intravenous gadodiamide contrast was administered to define EOM tendons anterior to the globe equator. Paths of EOMs, defined by their area centroids, were transformed into an oculocentric coordinate system. Sharp inflections in EOM paths in secondary and tertiary gaze positions defined pulley locations which were then correlated with gaze direction and compared with theoretical predictions.

RESULTS. Rectus pulley positions were consistent with a central primary position. In tertiary gaze positions, each of the four rectus pulleys translated posteriorly with EOM contraction and anteriorly with EOM relaxation by a significant ($P < 0.02$) amount predicted by the APH, but more than 100 times greater than the translation predicted by a passive pulley model.

CONCLUSIONS. The APH prediction of coordinated anteroposterior shifting of EOM pulleys with gaze is quantitatively supported by changes in EOM path inflections among tertiary-gaze positions. Human rectus pulleys move to shift the ocular rotational axis to attain commutative behavior of the ocular motor plant. (*Invest Ophthalmol Vis Sci.* 2002;43:2179–2188)

The orbital connective tissues in the region of the extraocular muscles (EOMs) have long been recognized to be stereotypic in composition and organization.^{1–3} Indeed, the idea that these tissues might control EOM paths was proposed as long ago as the late 19th century, when the French term “poulie” was applied to their function.⁴ Even more classic is the notion that the EOMs insert not only on the globe through their tendons, but, from the time of Bonnet, it has been recognized that EOMs also attach to the enveloping connective

tissues of the Tenon capsule.^{1,4} Later histologic examinations revealed that the orbital layer of each rectus EOM terminates on the connective tissue.^{5,6} Nevertheless, the concept of control of rectus EOM paths by connective tissues was largely neglected until recently when computed radiographic tomography⁷ and magnetic resonance imaging (MRI) began to be used to investigate the effect of gaze shifts on EOM paths.^{8–14} These studies have repeatedly confirmed relative stability of posterior EOM paths despite large horizontal and vertical gaze shifts.

Imaging in living subjects now shows that each rectus EOM does not pull toward its classic anatomic origin in the annulus of Zinn. Instead, EOM force is directed toward a much more anteriorly located and mechanically stable connective tissue structure called a pulley.¹⁵ Each rectus pulley consists of an encircling sleeve and ring of collagen located near the globe equator in the Tenon fascia,¹⁵ coupled to the orbital wall, adjacent EOMs, and equatorial Tenon fascia by sling-like bands containing collagen, elastin, and richly innervated smooth muscle.¹⁶ Pulleys deflect rectus and inferior oblique EOM paths in a manner qualitatively similar to the deflection of the superior oblique tendon path by the trochlea, although the rectus pulleys are less rigid. As might have been expected from the classically understood uniformity of orbital connective tissue structure,¹ the coronal plane location of each rectus pulley as determined by MRI is highly uniform in normal subjects.⁹ The global layer (GL) of each rectus EOM, containing about half of total EOM fibers,¹⁷ passes through the pulley and becomes contiguous with tendon to insert on the globe. The orbital layer (OL), containing the remaining roughly half of the EOM fibers, inserts on the pulley, not on the globe.^{17,18}

Rectus pulleys influence ocular kinematics, the rotational properties of the eye. Rotations of any three-dimensional (3-D) object are not mathematically commutative—that is, final eye orientation depends on the order of rotations.¹⁹ Angular velocity of a 3-D object differs from the rate of change of its orientation, being a complex function related to both the time derivative and the instantaneous eye orientation.^{20,21} Each combination of horizontal and vertical eye positions could, for an arbitrary solid object, be associated with an infinite number of torsional positions.²² The eye is constrained in its torsional freedom (with the head upright and immobile) by a relationship known as Donders' law,²³ stating that there is a unique torsional eye position for each combination of horizontal and vertical eye position.²⁰ Listing's law, a specific case of Donders' law, states that any physiologic eye orientation can be reached from any other by rotation about an axis lying in a single plane, the Listing plane.²⁴ Listing's law is satisfied if, for any eye movement, the velocity axis of ocular rotation shifts by exactly half of the shift in ocular orientation.²¹ This is the so-called Listing's half-angle rule.

Qualitative evidence of posterior shifts of the pulley tissues during rectus EOM contraction obtained in humans by the MRI-motivated proposal of the active pulley hypothesis (APH).¹⁸ The APH states that rectus pulleys move to regulate ocular kinematics and is considered herein to consist of two postulates: The coordinated control postulate of the APH accounts for kinematics conforming to Listing's half-angle rule by

From the Departments of ¹Ophthalmology and ³Neurology, University of California, Los Angeles, Los Angeles, California; and the ²Department of Ophthalmology, Okayama University Medical School, Okayama, Japan.

Supported by National Eye Institute Grant EY08313 (JLD). JLD is the recipient of a Research to Prevent Blindness Lew R. Wasserman merit award and is Laraine and David Gerber Professor of Ophthalmology at the University of California, Los Angeles.

Submitted for publication August 20, 2001; revised October 24, 2001 and January 4, 2002; accepted January 24, 2002.

Commercial relationships policy: N.

The publication costs of this article were defrayed in part by page charge payment. This article must therefore be marked “advertisement” in accordance with 18 U.S.C. §1734 solely to indicate this fact.

Corresponding author: Joseph L. Demer, Jules Stein Eye Institute, 100 Stein Plaza, UCLA, Los Angeles, CA 90095-7002; jld@ucla.edu.

supposing pulley movements along the EOM axis. The postulate states that, in an oculocentric coordinate system, rectus pulley location is maintained in a constant relationship with the EOM's scleral insertion, so that the distance from the pulley to globe center is equal to the distance from globe center to insertion. By this relationship, the velocity axis produced by EOM contraction shifts by half the change in ocular orientation. Such half-angle behavior implements a linear ocular motor plant that is effectively commutative (in the mathematical sense) with respect to ocular rotations.²⁵ The differential control postulate of the APH was proposed to account for ocular motor kinematics such as observed during the vestibulo-ocular reflex (VOR)²⁶ and convergence²⁷⁻²⁹ not conforming to the classic description of Listing's law. The differential control postulate proposed that differential innervation in rectus OLs and GLs, oblique EOM OLs, or orbital smooth muscle, separately may move the rectus pulleys differently from the travel of their scleral insertions¹⁸ or even in directions transverse to the EOM axis,^{14,30,31} to alter ocular kinematics. The original proposal of differential control of rectus pulleys supposed larger anteroposterior shifts during the VOR than during visually guided eye movements.¹⁸ Although differential control of pulleys as originally proposed no longer appears to be a tenable explanation for the steady state VOR during low frequency head rotation,³² pulley repositioning transverse to the rectus EOM axes appears to occur during convergence,^{30,31} albeit in different directions than originally proposed.¹⁸

Given the precise quantitative implications of rectus pulley position, mere qualitative evidence of pulley motion along EOM axes is insufficient. A test of either postulate of the APH must be quantitative, because the details are central to determination of the relative contributions of neural and mechanical factors to ocular motor control.³² At present, MRI cannot directly resolve the location of each human rectus pulley ring sufficiently to determine gaze-related changes with adequate precision. However, rectus paths can be followed sufficiently anterior in the orbit by high resolution MRI to determine the discrete inflections produced by the pulleys. This method was used for the secondary gaze positions, either horizontal or vertical, to confirm that the anteroposterior locations of all the rectus pulleys were consistent with the average orientation of the Listing plane.¹⁴ The coordinated control postulate of the APH predicts large anteroposterior shifts in pulley locations in tertiary gaze positions, positions containing both horizontal and vertical components.¹⁸ Alternatively, the Orbit 1.8 computational simulation of orbital mechanics, a detailed biomechanical model that implements passive EOM pulleys, allows pulleys to move only under passive elastic tension and thus predicts negligible anteroposterior shifts of rectus pulleys.³³ Although technically difficult, it is now possible to demonstrate EOM paths anterior to the pulleys in these eccentric gaze positions using high resolution, surface coil MRI and paramagnetic contrast.³⁴

The present study was conducted to measure accurately the EOM pulley locations in secondary and tertiary gaze positions, allowing quantitative comparison with predictions of the coordinated control postulate of the APH versus the alternative supposition of passive pulley behavior. The current experiment did not address the differential control postulate.

METHODS

Subjects

Eight adult volunteers were recruited by advertisement and gave written informed consent according to a protocol conforming to the Declaration of Helsinki and approved by the Human Subject Protection Committee at the University of California, Los Angeles. All volunteers

underwent complete eye examinations verifying normal corrected vision, normal ocular versions, orthotropia in all gaze positions, and stereopsis of 40 arcsec by Titmus testing.

Magnetic Resonance Imaging

High-resolution, T₁-weighted MRI was performed with a 1.5-T scanner (General Electric Signa; Milwaukee, WI). Crucial aspects of this technique, described in detail elsewhere, include use of a dual-phased surface coil array (Medical Advances, Milwaukee, WI) to improve signal-to-noise ratio and fixation targets to avoid motion artifacts.¹⁴ Initially, a localizer axial scan was obtained at 3-mm thickness using a 256 × 192 matrix over a 10-cm² field of view. Contiguous MRI images along the axis of the right orbit were obtained with 2-mm slice thickness, using a 256 × 256 matrix over an 8-cm² field of view, giving pixel resolution of 313 μm. Some of volunteers received the intravenous paramagnetic MRI contrast agent (gadodiamide, 0.1 mmol/kg) to improve the contrast of EOMs against connective tissue in the anterior orbit.³⁴

During imaging, subjects fixated small, individually illuminated, afocal targets delivered by a fiberoptic system mounted on the transparent faceplate of the surface coil array. Imaging was initially performed in central gaze, as well as in secondary positions of abduction, adduction, supraduction, and infraduction. Tertiary-gaze positions of supraducted abduction, infraducted abduction, supraducted adduction, and infraducted adduction were attained by presentation of the fixation target at the maximum eccentricities that could be maintained for the 3.5-minute duration of each scan. The actual eccentricities attained varied among subjects because of facial anatomy, but were measured in each case. For all adducted gazes, the fixation target was presented to the non-scanned fellow eye, because the nasal bridge and surface coil over it occlude a highly adducted target presentation to the scanned eye. One subject underwent complete imaging on two occasions, one without and the other with gadodiamide contrast.

Analysis

Digital MRI images were transferred to computer (Macintosh; Apple Computer, Cupertino, CA), converted into 8-bit tagged image file format (TIFF) using locally developed software, and quantified using NIH Image (Wayne Rasband, National Institutes of Health; available by file transfer protocol [FTP] from zippy.nimh.nih.gov or on floppy disc from NTIS, Springfield, VA, catalog number PB95-500195GEI).

In each of the MRI scans obtained, the location of each rectus EOM was described by a single point in each image plane using the "area centroid" function of the NIH Image program (Fig. 1). The area centroid of a cross-section is equivalent to the center of gravity of a shape of uniform density and thickness. Next, approximating the globe as spherical, its 3-D center was determined to subpixel resolution in scanner coordinates, by using curve fitting to cross-sectional images of the globe, as previously described.¹⁴ Rectus EOM positions were then translated to place the 3-D coordinate origin at the computed center of the globe. After data were transformed, the scanner coordinates were scaled to millimeters and were then scaled to normalize each globe to the measured average diameter of 24.3 mm found by MRI in an earlier study of normal subjects.¹⁴ Displacement of the globe-optic nerve junction from its position in central gaze was used to estimate ocular rotation, as previously described.¹⁴ For tertiary gaze positions, ocular rotation was measured using the Fick rotation sequence, with horizontal followed by vertical globe rotation. The central gaze target was chosen to approximate straight ahead gaze, and other gaze positions were measured relative to this position.

Because of low contrast with adjacent tissues, it was not possible in every gaze position of every subject to identify EOM cross-sections clearly in every image plane. To determine inflections in EOM paths in secondary or tertiary vertical gaze positions, we analyzed only those orbits for which there were complete image sets and inflection points in multiple gaze positions.

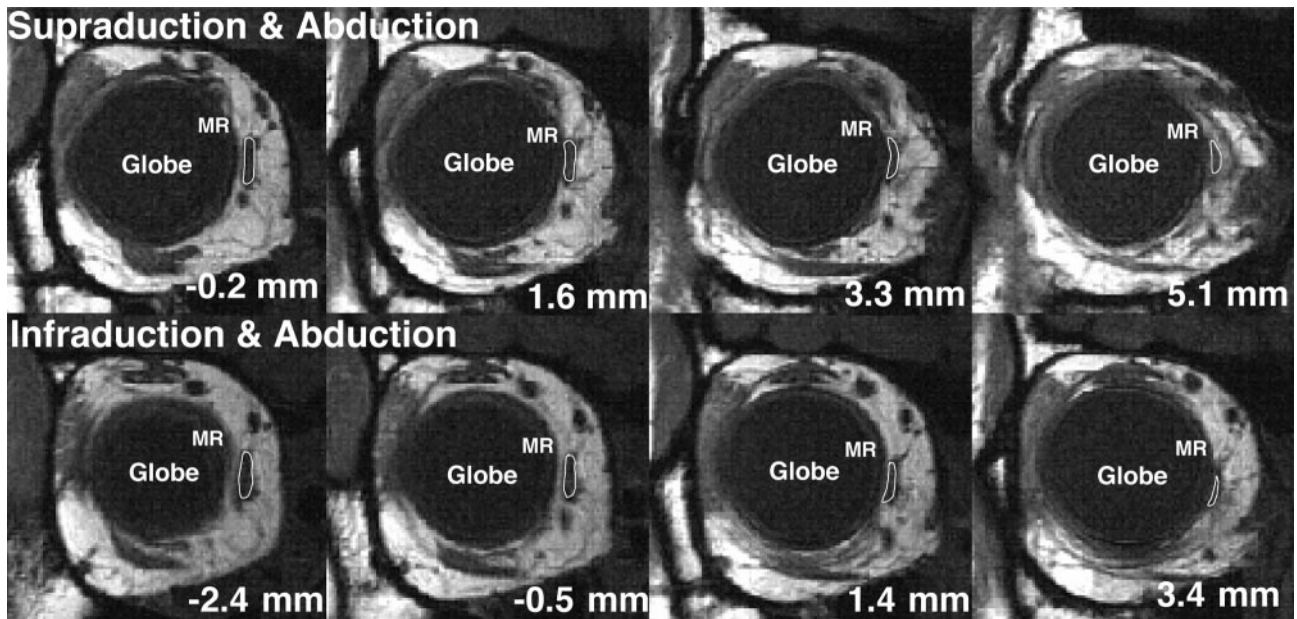


FIGURE 1. Magnetic resonance images in quasicoronal planes near the globe equator in the tertiary-gaze positions of supraducted abduction and infraducted abduction. The belly and tendon of the MR is outlined in white. The area centroids represent geometric centers of the areas outlined and were used to determine MR path. Numbers indicate the distance anterior to globe center in the normalized coordinate system. Anterior to globe center (right side), images show a superior shift of the MR tendon in elevation, with an inferior shift in depression.

Inflections were determined using piece-wise linear regression on EOM mean area centroid coordinates (Fig. 2).¹⁴ The data set representing the length of each EOM was divided into all possible combinations of anterior and posterior parts sequentially, beginning from the posterior orbit. Linear regressions and corresponding coefficients of variation (r^2) were then computed separately for the two parts, anterior and posterior, until all possible parsings of anterior and posterior data points were analyzed (Fig. 3). The best estimate of the inflection point for each EOM was taken to be the intersection of the two regressions with the highest summed coefficients of variation. This procedure

avoided subjective bias in determination of inflection points, but always identified inflections that appeared subjectively reasonable in comparison with graphed EOM paths. Because this procedure uses the entire data set to estimate the inflection point, it has anteroposterior resolution better than the MRI image thickness of 2 mm. The inflection was taken to represent the functional location of the involved pulley.

This procedure resulted in data pairs consisting of a gaze position and a pulley position. Gaze positions were deliberately varied through the nine target positions within subjects, and also varied among subjects. After pooling data across subjects for each of the four EOMs, gaze and pulley positions were graphed and compared by linear regression. These graphs and regressions were compared with the predictions of the APH, accounting for the approximately 22° temporal orientation of the orbital axis relative to the standard coordinate system.

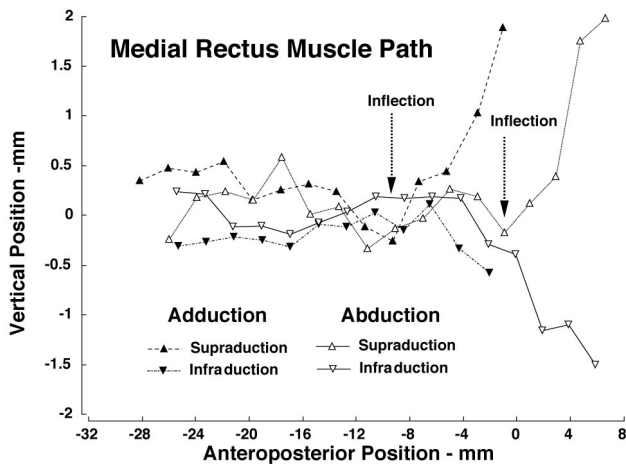


FIGURE 2. Path of the MR of a representative subject in the four tertiary-gaze positions. The inflection (arrow) in the MR path with vertical gaze indicates the pulley's location. Note the posterior location of the path inflection in adduction and anterior location in abduction. A linear trend due to a 10° upward orbital orientation relative to the coordinate system was uniformly removed from MR paths for graphical clarity. The following gaze positions were imaged: 21.6° abduction with 14.6° supraduction; 20.0° abduction with 19.8° infraduction; 36.6° adduction with 20.5° supraduction; and 16.4° adduction with 6.7° infraduction.

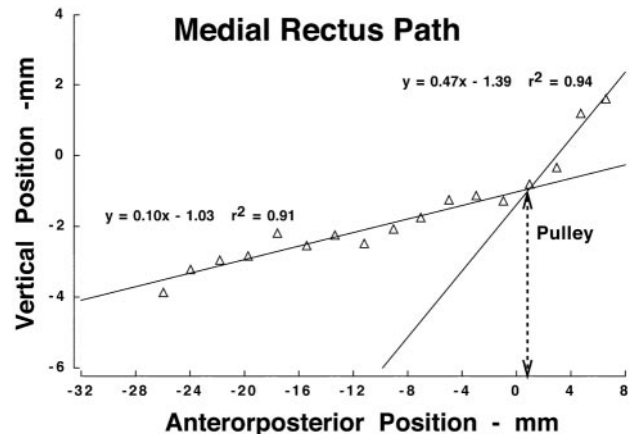


FIGURE 3. Path of the MR of a representative subject in supraducted abduction illustrating determination of anteroposterior pulley location by piece-wise linear regression. The summed coefficient of determination (r^2) was maximized when the most anterior four data points were assigned anterior to the pulley, and the remainder assigned posterior to it. Intersection of the resultant two linear regressions provided the best estimate of pulley location (double-ended broken arrow).

TABLE 1 Gaze Angles during MRI Scanning (mean \pm SD)

Gaze Position	Angle of Supraduction (deg)	Angle of Abduction (deg)
Infraduction	-23.9 ± 2.4	2.2 ± 6.4
Supraduction	20.3 ± 4.0	13.0 ± 11.4
Abduction	2.4 ± 5.2	22.3 ± 5.5
Adduction	-2.8 ± 5.4	-29.2 ± 2.2
Infraducted Adduction	-20.6 ± 8.1	-21.7 ± 6.9
Supraducted Adduction	19.8 ± 6.7	-23.8 ± 6.7
Infraducted Abduction	-19.0 ± 5.6	14.9 ± 5.2
Supraducted Abduction	15.0 ± 5.9	21.3 ± 8.4

RESULTS

The eight normal subjects ranged in age from 21 to 59 years (mean, 33 ± 12 [SD]). Mean globe diameter determined from MRI was 24.7 ± 1.2 mm (range, 22.4–25.9). Mean gaze positions used in imaging are summarized in Table 1. Axial plane imaging with the central target presented to the right eye confirmed the absence of binocular convergence.

Centroids were determined for each of the rectus EOMs (Fig. 1) and shifted with gaze in the anterior orbit. The locations of rectus pulleys were identifiable from discrete inflections in rectus EOM paths, determined by centroids, in secondary and tertiary gaze positions. In tertiary-gaze positions, these inflections moved posteriorly during EOM contraction and anteriorly during relaxation. Figure 2 displays representative data from one subject showing average vertical area centroid positions of the MR muscle along the anteroposterior orbital axis, with zero referenced to globe center. An upward trend in MR path due to orbital orientation in the skull has been uniformly removed from each path for graphic clarity. Imaging was performed in the four tertiary gaze positions. If no pulley had existed, the MR path would have followed an approximately straight line from the orbital apex to the vertically displaced MR insertion in each tertiary gaze position. The posterior MR path was little changed by gaze position, exhibiting only small parallel shifts indicative of globe translation.¹⁴ There was a discrete inflection in MR path, indicative of the MR pulley, however, anterior to which the MR followed the vertical gaze direction toward the scleral insertion. As may be seen in Figure 2, in 27° mean adduction the MR path inflection produced by vertical gaze was approximately 6 to 9 mm posterior to globe center, whereas in 21° mean abduction the same inflection occurred 0 to 4 mm posterior to globe center, which indicates anterior displacement of the MR pulley with abduction.

By inspection of EOM centroid plots at an anteroposterior resolution equal to the 2-mm thickness of the image planes (Fig. 2), EOM path inflections appeared sharp. Locations of pulley inflections were estimated with greater precision using the intersections of piece-wise linear regressions, as illustrated in Figure 3. This allowed all the path data to contribute to the estimates and avoided subjective bias. A separate measure of anteroposterior pulley position was obtained for each tertiary-gaze position, because both the horizontal and vertical components typically varied somewhat.

Pooling all the data for which pulley positions were available, the relationship of anteroposterior pulley position to horizontal gaze angle is displayed for the MR in Figure 4. Data were available for the gaze range of 35° adduction through 35° abduction, for which the MR pulley moved from approximately 13 mm posterior to 1 mm anterior to globe center. A linear regression through these data points yielded a slope of 4.51 ± 0.57 deg/mm (SE; $n = 36$) of pulley shift that was

significantly different from zero ($P < 0.0001$) and accounted for 65% of the variance. Zero degrees of horizontal gaze, the presumptive primary position, corresponded by interpolation to a pulley location 5.3 mm posterior to globe center.

Because of difficulties in distinguishing the lateral rectus (LR) from adjacent soft tissues, fewer total determinations of LR pulley position could be made than for the medial rectus (MR), encompassing a smaller range of gaze from 10° abduction to 30° adduction. Larger amounts of abduction resulted in greater obscuration of the LR by the lacrimal gland and adjacent soft tissues. Anteroposterior LR pulley positions are pooled and plotted as a function of horizontal gaze angle in Figure 5. This plot is almost a mirror image of that in Figure 4 for the MR, with the LR pulley moving from 13 mm posterior to globe center in abduction to 3 mm posterior to globe center in adduction. A linear regression through these data points yielded a slope of -3.36 ± 1.16 deg/mm ($n = 11$) of pulley shift that was significantly different from zero ($P = 0.018$) and accounted for 48% of the variance. Zero degrees of horizontal gaze, the presumptive primary position, corresponded by interpolation to a pulley location 10.2 mm posterior to globe center.

Pooling all the data for which pulley positions were available, the relationship of anteroposterior pulley position to horizontal gaze angle is displayed for the superior rectus (SR) in Figure 6. Data are available for the gaze range of 25° supraduction through 30° infraduction, for which the SR pulley moved from approximately 14 mm posterior to 3 mm posterior to globe center. A linear regression through these data points yielded a slope of -5.47 ± 0.97 deg/mm ($n = 13$) of pulley shift that was significantly different from zero ($P = 0.0001$) and accounted for 74% of the variance. Zero degrees of horizontal gaze, the presumptive primary position, corresponded by interpolation to a pulley location 9.2 mm posterior to globe center.

With all the data pooled for which pulley positions were available, the relationship of anteroposterior pulley position to horizontal gaze angle is displayed for the IR in Figure 7. Data

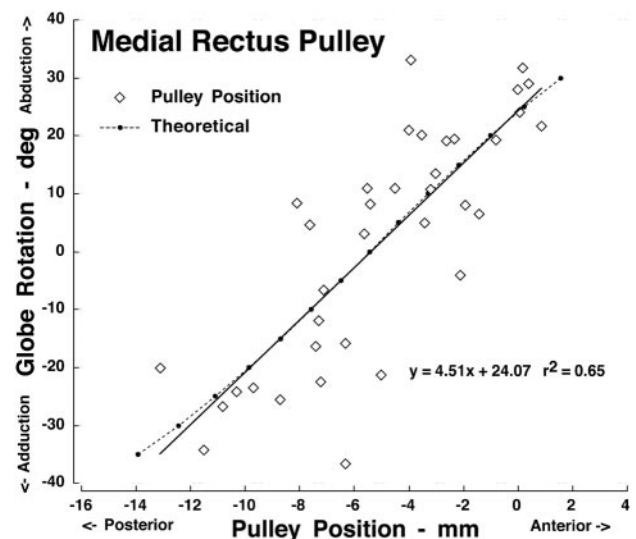


FIGURE 4. Relationship of horizontal gaze angle to anteroposterior position of the MR pulley. Data were pooled for all subjects, with each point determined from a set of contiguous MRI images in one gaze position that inflected the MR path. Abscissa zero is referenced to globe center. Solid line: linear regression through data points with slope significantly differing from zero ($P < 0.0001$). Dotted line: MR pulley position predicted by the APH. See the Discussion section and Figure 8 for theoretical details.

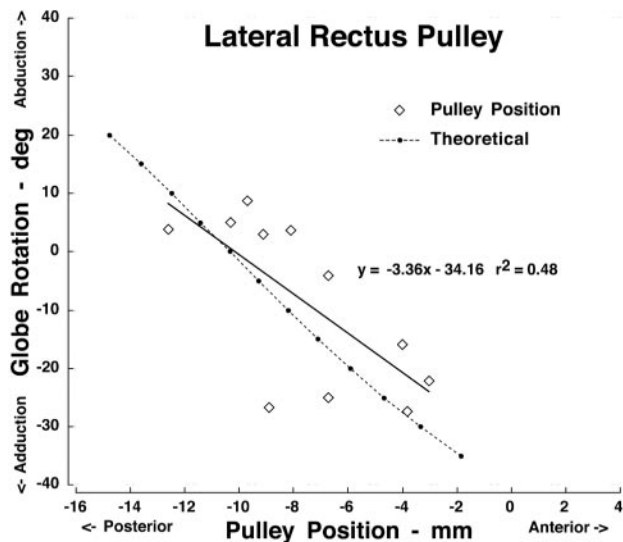


FIGURE 5. Relationship of horizontal gaze angle to anteroposterior position of the LR pulley. Data were pooled for all subjects, with each point determined from set of contiguous MRI images in one gaze position that inflected the LR path. Abscissa zero is referenced to globe center. *Solid line*: linear regression through data points with slope significantly differing from zero ($P = 0.017$). *Dotted line*: LR pulley position predicted by the APH. See the Discussion section and Figure 8 for theoretical details.

are available for the gaze range of 30° infraduction through 30° supraduction, for which the IR pulley moved from approximately 13 mm posterior to 3 mm anterior to globe center. A linear regression through these data points yielded a slope of 2.72 ± 0.47 deg/mm ($n = 30$) of pulley shift that was significantly different from zero ($P < 0.0001$) and accounted for 55% of the variance. Zero degrees of horizontal gaze, the presumptive primary position, corresponded by interpolation to a pulley location 4.2 mm posterior to globe center.

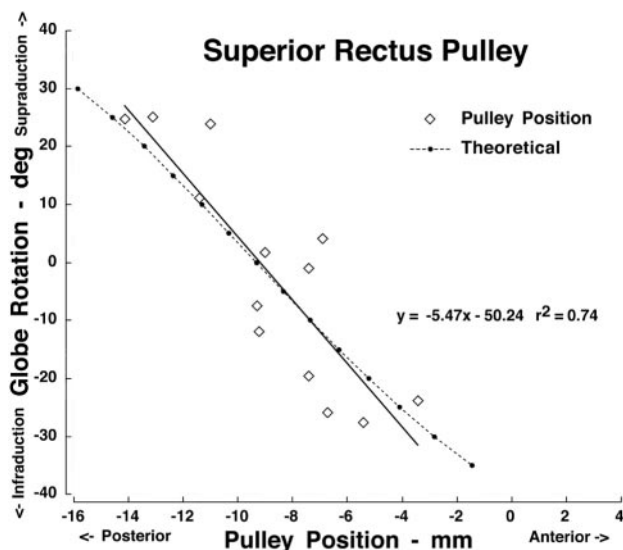


FIGURE 6. Relationship of vertical gaze angle to anteroposterior position of the SR pulley. Data were pooled for all subjects, with each point determined from set of contiguous MRI images in one gaze position that inflected the SR path. Abscissa zero is referenced to globe center. *Solid line*: linear regression through data points with slope significantly differing from zero ($P = 0.0001$). *Dotted line*: SR pulley position predicted by the APH. See The Discussion section and Figure 8 for theoretical details.

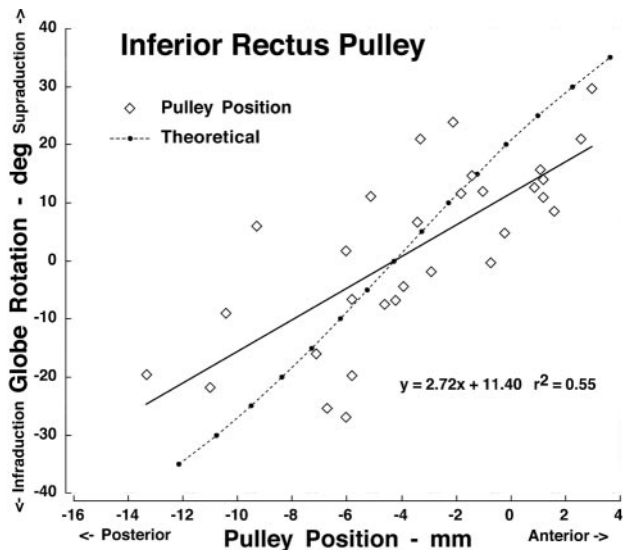


FIGURE 7. Relationship of vertical gaze angle to anteroposterior position of the IR pulley. Data were pooled for all subjects, with each point determined from set of contiguous MRI images in one gaze position that inflected the IR path. Abscissa zero is referenced to globe center. *Solid line*: linear regression through data points with slope significantly differing from zero ($P < 0.0001$). *Dotted line*: IR pulley position predicted by the APH. See the Discussion section and Figure 8 for theoretical details.

DISCUSSION

Support for Coordinated Control Postulate

Using careful MRI technique, including intravenous paramagnetic contrast, the anteroposterior locations of discrete rectus EOM path inflections associated with secondary- and tertiary-gaze positions could be determined in eight normal subjects. The 2-mm thickness of each MRI plane imposed this level of precision on measurements from individual images. Determination of EOM paths, however, from two-part regression on EOM centroid data from complete sets of 17 image planes improved anteroposterior precision to better than the 2-mm slice thickness. Pooling of data from multiple subjects further improved precision. Even without these precautions, however, the individual subject data were consistent with the group data in all essential regards. For each rectus EOM, a discrete inflection moved significantly posteriorly during EOM contraction and anteriorly during relaxation. These changes in path inflections are interpreted as anteroposterior shifts in the rectus EOM pulleys.

Histologic examination of serially sectioned human orbits indicates that the pulley regions consist of connective tissue sleeves of varying thickness surrounding the EOMs over an anteroposterior extent of approximately 10 mm.¹⁵ Although more focal, ringlike condensations of connective tissue within pulleys can be identified,^{16,18} direct morphologic examination of somewhat distributed orbital tissues, even in vivo by MRI, cannot provide exact locations for the biomechanically functional pulleys. Functional pulley locations are defined by the sharp inflections they confer on EOM paths in secondary- and tertiary-gaze positions.¹⁴ The rotational axis of an EOM is perpendicular to the average path of the EOM segment connecting the pulley inflection with the scleral insertion. Thus, linear regressions of anterior EOM paths by MRI provide the biomechanically relevant information on the direction of EOM action that is unavailable even from ideal direct study of connective tissues alone. Although direct imaging of pulley connective

tissues is not definitive for evaluation of the role of pulleys in ocular kinematics, direct imaging of horizontal rectus pulley components is consistent with pulley movements inferred from EOM paths.¹⁸ This qualitative behavior is a novel finding predicted by the coordinated control postulate of the APH,¹⁸ but may also be consistent with more general concepts of EOM connective tissue sleeves.

The coordinated control postulate of the APH is specific, however, in predicting that during visually guided eye movements, each rectus EOM pulley would move anteroposteriorly as if locked to the sclera. This axial mobility is predicted for visually guided eye movements in the nonconverged state, despite the observation that in the directions perpendicular to the EOM axis, the pulley remains highly stable in the orbit while the posterior sclera moves beneath it. Quantitative interpretation of this prediction requires conversion of the ocular relationship to the coordinate system in which the data were collected: one centered on the globe but rotationally referenced to cranial landmarks.¹⁴ The geometry is summarized in Figure 8. Let R = globe radius. Primary position is typically displaced somewhat from central gaze. In primary position, the LR pulley is thus located distance $X_0 = R \tan \theta_0$ posterior to globe center in the standard coordinate system, where θ_0 is the polar displacement of the LR pulley from the reference position. Primary position pulley location X_0 was directly determined from the horizontal axis intercept of linear regressions to the data for each EOM. In abduction, the LR pulley moved posteriorly to distance $X_{abd} = R \tan \theta_{abd}$ in the standard coordinate system, where θ_{abd} is the polar displacement of the LR

pulley. The net posterior displacement of the LR pulley ΔX resulting from abducting to angle θ_{abd} is thus given by

$$\Delta X = X_{abd} - X_0 = R \tan \theta_{abd} - R \tan \left[\arctan \left(\frac{X_0}{R} \right) \right]$$

For the vertical rectus EOMs, an additional trigonometric projection was made for the roughly 22° temporal orientation of the EOM axes.

Using the equation, predicted anteroposterior pulley position was computed and superimposed on the data in Figures 4 to 7. Note in Figures 4 and 6 that the linear regressions through the data almost superimpose the prediction of the coordinated control postulate of the APH. Although the slope of the regression for the LR (Fig. 5) and IR (Fig. 7) pulleys differed modestly from the theoretical prediction, the data still corresponded well to the prediction. The coordinated control postulate—rectus pulley repositioning corresponding to Listing’s half-angle behavior—thus has been quantitatively supported to the limit of precision of the MRI technique for each of the four EOMs.

Evidence against Passive Pulley Movements

The finding that, during visually guided fixations in the nonconverged state, rectus pulleys move anteroposteriorly with ocular rotation as if they were in fixed relationship with the globe naturally raises the possibility of the trivial explanation that the pulleys may be directly attached to the globe. Several lines of evidence exclude this possibility. First, MRI shows EOM paths at the pulley inflections to be widely separated from the sclera,³⁵ in a region where direct histologic examination shows no significant connective tissues in continuity with the globe. The posterior globe in the region of the pulleys is separated from the adjacent Tenon fascia by a bursalike space.¹⁵ Second, transverse to the EOM axes, rectus pulleys are highly stable in the orbit, despite large horizontal and vertical gaze shifts.^{8-12,15,36} Because pulleys are posterior to the center of globe rotation, they could not remain stable in the orbit if they were firmly adherent to the highly mobile globe underlying them. Third, division of all musculoglobal tissue connections during strabismus surgery has been demonstrated by MRI to have only a minimal effect on the coronal plane location of the rectus pulleys.³⁶ This was the first clear evidence that rectus EOM paths are controlled, not by musculoglobal couplings, but instead by orbitally coupled pulleys. The findings have been confirmed more recently, even after transposition surgery that involves surgical division of all musculoglobal attachments.³⁷

The high stiffness of pulley couplings to the orbital rim responsible for the general stability of rectus paths also works against any sort of passive anteroposterior displacement of the pulleys. The Orbit 1.8 computational simulation of orbital biomechanics implements pulleys passively suspended from the orbit at high stiffness (40 g/mm) to achieve the observed high stability of rectus EOM paths in the coronal plane.³³ With this passive implementation, Orbit 1.8 predicts for the MR pulley a maximum anteroposterior shift of only 0.1 mm over the ±35° horizontal gaze range that produced the 14-mm anteroposterior shift observed in this study. This discrepancy of more than two orders of magnitude between passive and active pulley behavior highlights the necessity of powerful muscular activity to position rectus pulleys. Finally, the mere existence of an EOM pulley does not necessarily obligate it to move with gaze shifts by the same distance as the nearby sclera, and not all EOM pulleys do so. The inferior oblique muscle has a pulley that moves anteroposteriorly with IR vertical gaze, but by only half the travel distance of the IR insertion and adjacent sclera.³⁸

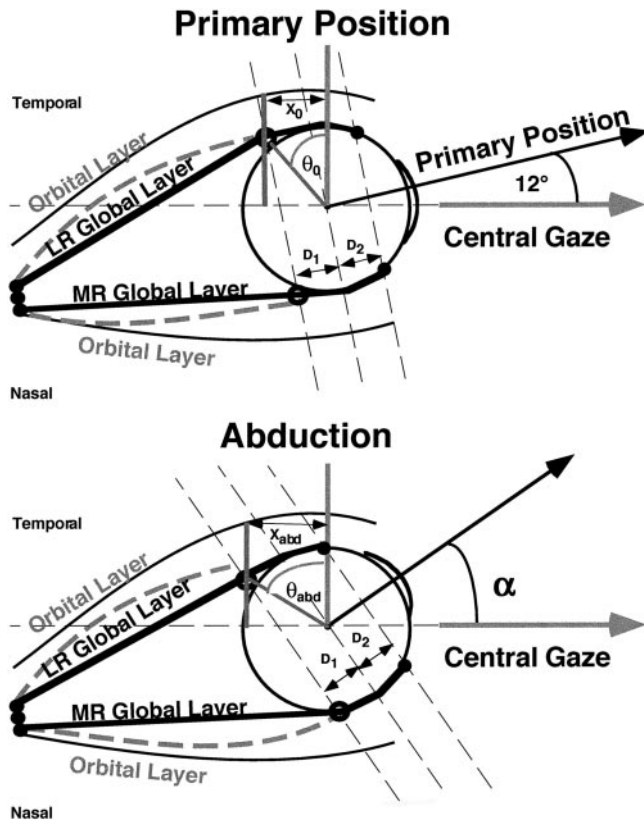


FIGURE 8. Horizontal rectus pulley movement with gaze as predicted by APH. Listing’s half-angle rule is satisfied when $D_1 = D_2$ in oculo-centric coordinates, requiring the horizontal rectus pulleys to move as if fixed to the globe’s circumference. Primary position may differ from central gaze, in this case by approximately 12°. See the Discussion section for computation of predicted pulley positions.

Could the anteroposterior shifts of pulleys along rectus EOM axes be attributable to passive forces exerted by the posterior pressure of EOM insertions alone? Qualitatively, this may appear to be a possibility. However, the data presented herein confirm that the insertions remain more than 16 mm from the pulleys along the ocular circumference, quite far to exert significant compressive force on the pulley. Except after surgical manipulations such as retroequatorial myopexy that are designed to cause the scleral insertions to mechanically interfere with the pulleys,¹³ mechanical pressure from the insertions on the pulleys would seem precluded. Rectus paths are bowed outward away from the orbital center, more during relaxation than during contraction.⁸ Although this effect has been attributed to hydrostatic pressure on compartmentalized orbital fat,⁷ a greater contribution to this effect is likely to come from the elastic suspensions of the pulleys that run radially and anteriorly toward attachments on the orbital rim.³⁵ Outward bowing is orthogonal to the anteroposterior movement of the rectus pulleys documented in this study, and so could, at most, convert only a small fraction of motion of the globe circumference into pulley translation.

Differential Effort in EOM Laminae

The current data show that under the current experimental conditions of nonconverged visual fixation, pulleys nevertheless move anteroposteriorly in one-to-one correspondence with the rectus insertions. Evidence suggests that posterior pulley movements arise from active tension of rectus EOMs on their respective pulleys. Could this effect be simply due to the classically recognized attachment of the connective tissue sleeves to the EOMs themselves? In a broad sense, the answer seems affirmative. The sleeves are adherent to the EOMs, and passive forces alone are inadequate to account for the pulley movements observed in this study. However, recent anatomic studies provide further insight into the nature of the insertion of rectus EOMs on their connective tissue sleeves. Mammalian EOMs are bilaminar, consisting of an OL and GL.⁵ The OL of each rectus EOM in humans,^{17,18,34} monkeys,^{17,34} rabbits (Demer JL, Poukens V, unpublished data, 2002), and rats³⁹ inserts into connective tissue in its pulley sleeve but does not insert on the sclera. Rectus OLs in humans typically contain around 10,000 fibers, although individual numbers vary in rough proportion to the amount of connective tissue in each pulley.¹⁷ The OLs contain almost as many fibers as the GLs that do insert, through tendons, on the globe. This would appear to be a sufficient EOM mass to actively position the pulleys, especially considering the higher vascularity³⁴ and fatigue resistance of the OL compared with GL.^{17,34} Rectus OL fibers are oriented anteroposteriorly, appropriate to translate the pulleys in that direction. In cat, the most powerful and fatigue-resistant motor units of the LR muscle, comprising 27% of all units, consist of single neurons innervating fibers in both the orbital and global layers.⁴⁰ These bilayer motor units would command similar timing of contraction in the two layers, an arrangement facilitating coordinated control of pulley position.

Could GL fibers participate in the anteroposterior positioning of pulleys even though the GL does not directly insert on the pulley? Frictional drag of GL fibers passing through a pulley would tend to move it in the direction observed in the present study, even without a direct insertion, as would friction of OL fibers against GL fibers at their interface within the EOM. Some frictional interaction between OL and GL probably occurs. However, even if the OL and GL were assumed to contract identically and homogeneously, moving a pulley attached to their combined homogeneous mass somewhere along their anteroposterior extents, the observed Listing's half-angle kinematics could not be achieved. This is because contractile short-

ening of the EOM anterior to the pulley would move the insertion closer to the pulley during EOM activation, and allow the insertion to relax farther away from the pulley during relaxation. Both of these effects would reduce the anteroposterior movement of the pulley relative to the orbit and allow the pulley to move relative to the globe, contrary to the current observations of pulley behavior conforming to Listing's half-angle kinematics. The current precise confirmation of the predicted coordinated pulley movements casts serious doubt on traditional assumptions of homogeneous EOM structure and behavior, suggesting instead a degree of differential effort of the OL and GL, even during eye movements conforming to Listing's law. Differential effort is suggested by quasisagittal imaging in the plane of the IR during vertical gaze shifts,³⁰ in which the two layers can be separately resolved to show greater thickening of the OL than GL in infraction. Even under static conditions, there is no biomechanical reason to expect that the stiffness of a pulley suspension, which plausibly might approximate a linear spring, should be equal to the rotational load on the globe, which by contrast varies in a complex way with eye position.⁴¹ The EOM effort devoted to positioning the pulley should thus be expected to differ from its effort in rotating the globe, even if equal movements are ultimately achieved. Selective electromyography (EMG) in the OL and GL of humans shows different recruitment thresholds in the two layers,⁴² again supporting the concept of differential effort.

Implications for Ocular Motor Control

Before pulleys were known, Listing's law was presumed to be implemented entirely by complex neural commands to the EOMs, despite absence of an identifiable neural substrate for this behavior. In the superior colliculus, saccades are encoded as the two-dimensional (2-D) rate-of-change of eye orientation, implying that any computation of the third dimension, torsion, is accomplished downstream.^{25,43} Even in the oculomotor nucleus and rostral interstitial nucleus of the medial longitudinal fasciculus, saccadic burst commands are better correlated with rate-of-change of 3-D eye position than with angular eye velocity.^{43,44}

Pulleys form a mechanical substrate for behavior conforming to Listing's law and other aspects of ocular kinematics.^{18,25,45} Figure 8 is a top view of a schematic globe showing rectus EOMs and pulleys. If the distance from pulley to globe center (D_1) is equal to the distance from insertion to globe center (D_2), then (for small angles typical of the oculomotor range) the rotational axis tilts posteriorly by half the angle of the eye, as required by Listing's law. As demonstrated here, in tertiary gaze positions, pulleys shift within the orbit to maintain these relationships relative to the scleral insertions.¹⁸ Pulleys render horizontal and vertical eye position commands essentially commutative, simplifying central neural control,^{25,45} so that even a simple, 2-D control law suffices.⁴⁶

The pulley system does not always require conformity to Listing's law, which may be violated by explicit neural commands.²⁵ Noncommutative behavior of the oculomotor system, such as the VOR⁴⁷ and visual spatial localization,⁴⁸ would require explicit specification in the brain. When the head is rotated, Listing's law is violated by the VOR for which the velocity axis rotates from as much as approximately 25%⁴⁹ to as little as 0%^{50,51} of the ocular angle. A kinematically ideal VOR would have a rotation axis coincident with the head and independent of eye position, so as to optimally stabilize retinal images. Non-Listing VOR kinematics cannot be explained by coordinated or even differential anteroposterior shifts in rectus pulley locations.³² For the VOR, the oblique EOMs must play important roles. The oblique EOMs are configured to maintain

a half-angle behavior orthogonal to rectus half-angle behavior, apparently ideal for commanded violations of Listing's law,⁵² as during the VOR. Kinematics of the VOR are consistent with high gain pitch and yaw responses mediated by mechanisms consistent with the coordinated control postulate of the APH, but a lower gain roll response consistent with the observed behavior of the torsional VOR.⁵² Another instance of the VOR is static ocular counterrolling in response to maintained head tilt relative to gravity. Recordings from burst neurons in monkeys are compatible with torsional shift of rectus pulleys transverse to the EOM axes in the direction of ocular counterroll induced by static head tilt.⁵³ This pulley shift may be mediated by the oblique EOMs.³⁰

The coordinated control postulate of the APH has major implications for ocular dynamics.^{18,35} By implementing a linear plant, pulleys permit motor commands to the EOM GL to consist of the rate of change of desired eye orientation, and its simple mathematical integral.^{25,45} This simplifies the otherwise complex problem of matching the pulse to the step of saccadic innervation to avoid postsaccadic drift.²⁵ As a corollary, abnormal pulley locations are predicted to cause postsaccadic drift for saccades from secondary to tertiary gaze positions.²⁵ Because the mechanical loads on the OL and GL differ, coordinated control during saccades conforming to Listing's law should not be expected to be associated with either equal effort or identical neural commands in the OL and GL. Selective EMG recordings in the human MR GL demonstrated both a phasic pulse and tonic step of activity during saccades—the former necessary to drive the formidable viscous load imposed by the relaxing antagonist EOM, and the latter necessary to oppose the lesser elastic load as position is maintained.⁴² Recordings of tension at the insertions of simian horizontal rectus EOMs confirmed the presence of both saccadic pulses and steps.⁵⁴ In the human OL, however, EMG showed only a step of activity during saccades.⁴² The OL's mechanical load is likely to be dominated by elasticity of the attached pulley suspension. Collins has pointed out that the main load on an EOM attached to the globe is viscosity arising from the relaxing antagonist EOM.⁴² A phasic pulse of force in the OL is unnecessary to achieve brisk pulley motion against a mainly elastic load. However, this elastic loading by passive connective tissue requires that OL fibers maintain active tension throughout the oculomotor range to avoid slack. In contrast, GL fibers remain under tension, even when relaxed due to stretching by the antagonist EOM. Thus, to maintain coordinated control and identical movements of the pulley and globe under dynamic conditions such as saccades, the innervation to OL and GL must differ. The coordinated control postulate of the APH predicts that motor neurons preferentially innervating fibers in the OL should, during saccades, exhibit step, but not pulse, changes in activity. Many such "tonic" motor neurons have been found in the abducens and oculomotor nuclei.⁵⁵ Separate motor neurons projecting exclusively to the OL or GL have been demonstrated in the feline LR.⁴⁰

Differential Control

As pointed out earlier, even coordinated control of pulley movement requires differential EOM effort because of different static and dynamic loadings on pulley and globe. This implies a requirement for at least some differential neural commands to the OL and GL of each EOM, even during coordinated control. Beyond differential effort to achieve coordinated control, the APH also includes a second postulate, differential control. The postulated differential control supposes pulley movements in a direction or an amount different from ocular rotation. Movements of pulleys unrelated to ocular rotations were neither anticipated nor found in the current experiment, and the

present data are therefore not informative concerning the possibility of differential control. Alterations in EOM paths independent of horizontal and vertical eye position have been observed, however, during convergence,^{30,31} suggesting that differential control of pulley positions may exist. That possibility should be further investigated.

Primary Position

To assess rectus pulley positions as a function of gaze, it would have been ideal to use true kinematic primary eye position as the reference, defined as a zero-torsion normal to Listing's plane.⁵⁶ Unfortunately, even in the head-upright position, Listing's plane has considerable craniotopic variability among individuals,⁵⁷ and the plane shifts with head position⁵⁸ and variably with convergence, depending on the stimulus.^{59,60} The yaw orientation of Listing's plane has not been determined for the supine position used in the current experiment. Relative to a plane passing through globe center and tilted temporally by 12°, however, both the MR and LR pulleys were 7.8 mm posterior to globe center. This distance is consistent with the reported temporal tilt of the Listing plane in upright subjects. When the pulley position graphs for the MR (Fig. 4) and the LR (Fig. 5) are superimposed, they intersect 7.4 mm posterior to globe center. This distance is similar to the roughly 8-mm distance from globe center anterior to the MR and LR insertions, as required for half-angle behavior. It should be noted, however, that the current findings are independent of the chosen reference position. The graphs in Figures 4 and 5 would intersect approximately 8 mm posterior to globe center for any arbitrary rotational reference position consistently chosen for both graphs. It should also be noted that rectus EOM insertions are broad and often modestly slanted relative to the corneoscleral limbus,^{3,61} and therefore agreement to within 1 mm of measurements and a theory representing each EOM as a single point insertion is probably the best that can be expected.

The mean vertical (pitch) tilt of Listing's plane in upright humans is reportedly less variable than the horizontal, being on average tilted upward by 3° in upright subjects,⁵⁷ with little change in the supine position used in the current study.⁶² The vertical position chosen to be central for this study appeared natural, but was necessarily arbitrary. Relative to the cranium, the SR pulley was found to be 9.2 mm posterior to globe center, and the IR pulley 4.2 mm posterior. Relative to a plane passing through globe center and tilted superiorly by 12°, however, both the SR and IR pulleys were 6.7 mm posterior to globe center. When the pulley position graphs for the SR (Fig. 6) and the IR (Fig. 7) are superimposed, they intersect 7.5 mm posterior to globe center. This distance is also consistent with the approximately 8 mm distance from globe center anterior to the SR and IR insertions required for half-angle behavior, if the Listing plane were tilted superiorly by 12°. The origin of this presumed small upward tilt of the Listing plane is uncertain, but perhaps related to the near-viewing environment of the MRI scanner relative to the longer viewing distances used by other investigators.⁶² Nevertheless, as for the horizontal rectus EOMs, the current findings are independent of the chosen reference position. The graphs in Figures 6 and 7 would intersect at 7.5 mm posterior to globe center for any arbitrary rotational reference position consistently chosen for both graphs.

Implications for Models of the Ocular Motor Plant and Central Control

The quantitative consistency of the present data with the prediction of the coordinated control postulate of the APH validates the relatively novel assumption of a linear ocular motor plant used in recent dynamic models.^{25,32,45,63} Realistic dynamic models now cannot avoid this feature. Computational

models of binocular statics, such as the Orbit model,³³ should also implement moving pulleys conforming to Listing's half-angle behavior. Future studies of neural control of eye movements perhaps should involve study of EOM pulley behavior in addition to eye orientation. This is feasible by MRI in humans and possibly also in behaving animals.

Acknowledgments

The authors thank Nicolasa de Salles and Frank Henriquez for technical assistance, Huib Simonsz for providing the publication listed in reference 4, and Joel M. Miller for helpful suggestions regarding the concepts of coordinated and differential control.

References

- Koornneef L. Details of the orbital connective tissue system in the adult. *Acta Morphol Neerl Scand.* 1977;15:1-34.
- Koornneef L. The first results of a new anatomical method of approach to the human orbit following a clinical enquiry. *Acta Morphol Neerl Scand.* 1974;12:259-282.
- Fink WH. *Surgery of the Vertical Muscles of the Eye.* Springfield, IL: Thomas; 1962:37-121.
- Sappey PC. *Traite D'Anatomie Descriptive avec Figures Intercalees dans le Texte.* Paris: Delahaye et Lecrosnier; 1888.
- Porter JD, Baker RS, Ragusa RJ, Brueckner JK. Extraocular muscles: basic and clinical aspects of structure and function. *Surv Ophthalmol.* 1995;39:451-484.
- Spencer RF, Porter JD. Structural organization of the extraocular muscles. In: Buttner-Ennever J, ed. *Neuroanatomy of the Oculomotor System.* Amsterdam: Elsevier; 1988:33-79.
- Simonsz HJ, Harting F, de Waal BJ, Verbeeten BWJM. Sideways displacement and curved path of recti eye muscles. *Arch Ophthalmol.* 1985;103:124-128.
- Miller JM. Functional anatomy of normal human rectus muscles. *Vision Res.* 1989;29:223-240.
- Clark RA, Miller JM, Demer JL. Location and stability of rectus muscle pulleys inferred from muscle paths. *Invest Ophthalmol Vis Sci.* 1997;38:227-240.
- Clark RA, Miller JM, Rosenbaum AL, Demer JL. Heterotopic rectus muscle pulleys or oblique muscle dysfunction? *J Am Assoc Pediatr Ophthalmol Strabismus.* 1998;2:17-25.
- Clark RA, Miller JM, Demer JL. Displacement of the medial rectus pulley in superior oblique palsy. *Invest Ophthalmol Vis Sci.* 1998;39:207-212.
- Clark RA, Rosenbaum AL, Demer JL. Magnetic resonance imaging after surgical transposition defines the anteroposterior location of the rectus muscle pulleys. *J Am Assoc Pediatr Ophthalmol Strabismus.* 1999;3:9-14.
- Clark RA, Isenberg SJ, Rosenbaum SJ, Demer JL. Posterior fixation sutures: a revised mechanical explanation for the Faden operation based on rectus extraocular muscle pulleys. *Am J Ophthalmol.* 1999;128:702-714.
- Clark RA, Miller JM, Demer JL. Three-dimensional location of human rectus pulleys by path inflections in secondary gaze positions. *Invest Ophthalmol Vis Sci.* 2000;41:3787-3797.
- Demer JL, Miller JM, Poukens V, Vinters HV, Glasgow BJ. Evidence for fibromuscular pulleys of the recti extraocular muscles. *Invest Ophthalmol Vis Sci.* 1995;36:1125-1136.
- Demer JL, Poukens V, Miller JM, Micevych P. Innervation of extraocular pulley smooth muscle in monkeys and humans. *Invest Ophthalmol Vis Sci.* 1997;38:1774-1785.
- Oh SY, Poukens V, Demer JL. Quantitative analysis of extraocular muscle global and orbital layers in monkey and human. *Invest Ophthalmol Vis Sci.* 2001;42:10-16.
- Demer JL, Oh SY, Poukens V. Evidence for active control of rectus extraocular muscle pulleys. *Invest Ophthalmol Vis Sci.* 2000;41:1280-1290.
- Haslwanter T. Mathematics of three-dimensional eye rotations. *Vision Res.* 1995;35:1727-1739.
- Tweed D, Vilis T. Implications of rotational kinematics for the oculomotor system in three dimensions. *J Neurophysiol.* 1987;58:832-849.
- Tweed D, Vilis T. Geometric relations of eye position and velocity vectors during saccades. *Vision Res.* 1990;30:111-127.
- van den Berg AV. Kinematics of eye movement control. *Proc R Soc Lond B Biol Sci.* 1995;260:191-197.
- Donders FC. Physiological and pathological remarks on varying topics. IV: the movements of the human eye. *Strabismus.* 1999;7:175-181.
- Ruete CGT. Ocular physiology. *Strabismus.* 1999;7:43-60.
- Quaia C, Optican LM. Commutative saccadic generator is sufficient to control a 3-D ocular plant with pulleys. *J Neurophysiol.* 1998;79:3197-3215.
- Smith MA, Crawford JD. Neural control of rotational kinematics within realistic vestibuloocular coordinate systems. *J Neurophysiol.* 1998;80:2295-2315.
- van Rijn IJ, van den Berg AV. Binocular eye orientation during fixations: Listing's law extended to include eye vergence. *Vision Res.* 1993;33:691-708.
- Somani RAB, Desouze JFX, Tweed D, Vilis T. Visual test of Listing's law during vergence. *Vision Res.* 1998;38:911-923.
- Steffen H, Walker MF, Zee DS. Rotation of Listing's plane with convergence: independence from eye position. *Invest Ophthalmol Vis Sci.* 2000;41:715-721.
- Demer JL. The orbital pulley system: a revolution in concepts of orbital anatomy. *Ann NY Acad Sci.* 2002;956:17-32.
- Demer JL, Kono R, Wright W. Magnetic resonance imaging (MRI) of human extraocular muscles (EOMs) during asymmetrical convergence [abstract]. 2002 Annual Meeting Abstract and Program Planner accessed at www.arvo.org. Association for Research in Vision and Ophthalmology. Abstract 1915.
- Misslisch H, Tweed D. Neural and mechanical factors in eye control. *J Neurophysiol.* 2001;86:1877-1883.
- Miller JM, Pavlovski DS, Shaemeva I. *Orbit 1.8 Gaze Mechanics Simulation.* San Francisco: Eidactics; 1999.
- Oh SY, Poukens V, Cohen MS, Demer JL. Structure-function correlation of laminar vascularity in human rectus extraocular muscle. *Invest Ophthalmol Vis Sci.* 2001;42:17-22.
- Demer JL. Extraocular muscles. In: Jaeger EA, Tasman PR, ed. *Clinical Ophthalmology.* Vol. 1. Philadelphia: Lippincott; 2000:Chap 1.
- Miller JM, Demer JL, Rosenbaum AL. Effect of transposition surgery on rectus muscle paths by magnetic resonance imaging. *Ophthalmology.* 1993;100:475-487.
- Clark RA, Demer JL. Rectus extraocular muscle pulley displacement after surgical transposition and posterior fixation for treatment of paralytic strabismus. *Am J Ophthalmol.* 2002;133:119-128.
- Demer JL, Oh SY, Poukens V. Orbital layers of the oblique extraocular muscles (EOMs) insert on the orbital connective tissue system [ARVO Abstract]. *Invest Ophthalmol Vis Sci.* 2001;42(4):S517. Abstract nr 2781.
- Khanna S, Porter JD. Evidence for rectus extraocular muscle pulleys in rodents. *Invest Ophthalmol Vis Sci.* 2001;42:1986-1992.
- Shall MS, Goldberg SJ. Lateral rectus EMG and contractile responses elicited by cat abducens motoneurons. *Musc Nerve.* 1995;18:948-955.
- Miller JM, Robinson DA. A model of the mechanics of binocular alignment. *Comput Biomed Res.* 1984;17:436-470.
- Collins CC. The human oculomotor control system. In: Lennerstrand G, Bach-y-Rita P, ed. *Basic Mechanisms of Ocular Motility and Their Clinical Implications.* New York: Pergamon; 1975:145-180.
- Hepp K. Oculomotor control: Listing's law and all that. *Curr Opin Neurobiol.* 1994;4:862-868.
- van Opstal J, Hepp K, Suzuki Y, Henn V. Role of the monkey nucleus reticularis tegmenti pontis in the stabilization of Listing's plane. *J Neurosci.* 1996;16:7284-7296.
- Raphan T. Modeling control of eye orientation in three dimensions. I: role of muscle pulleys in determining saccadic trajectory. *J Neurophysiol.* 1998;79:2653-2667.
- Porrill J, Warren PA, Dean P. A simple control laws generates Listing's positions in a detailed model of the extraocular muscle system. *Vision Res.* 2000;40:3743-3758.

47. Tweed DB, Haslwanter TP, Happe V, Fetter M. Non-commutativity in the brain. *Nature*. 1999;399:261-263.
48. Smith ME, Crawford JD. Implications of ocular kinematics for the internal updating of visual space. *J Neurophysiol*. 2001;86:2112-2117.
49. Misslisch H, Tweed D, Fetter M, Sievering D, Koenig E. Rotational kinematics of the human vestibuloocular reflex. III: Listing's law. *J Neurophysiol*. 1994;72:2490-2502.
50. Misslisch H, Hess BJ. Three-dimensional vestibuloocular reflex of the monkey: optimal retinal image stabilization versus listing's law. *J Neurophysiol*. 2000;83:3264-3276.
51. Palla A, Straumann D, Obzina H. Eye-position dependence of three-dimensional ocular rotation axis orientation during head impulses in humans. *Exp Brain Res*. 1999;129:127-133.
52. Demer JL. Mechanical interactions of oblique extraocular muscles (EOMs) with actively controlled rectus pulleys maintain kinematics of linear oculomotor plant. *Soc Neurosci Abstr*. 2001;27:2071.
53. Scherberger H, Cabungcal J-H, Hepp K, et al. Ocular counterroll modulates the preferred direction of saccade-related pontine burst neurons in the monkey. *J Neurophysiol*. 2001;86:935-949.
54. Miller JM, Robins D. Extraocular muscle forces in alert monkey. *Vision Res*. 1992;32:1099-1113.
55. Henn V, Cohen B. Eye muscle motor neurons with different functional characteristics. *Exp Brain Res*. 1972;45:561-568.
56. Hausteil W. Considerations on Listing's law and the primary position by means of a matrix description of eye position control. *Biol Cybern*. 1989;60:411-420.
57. Haslwanter T, Curthoys IS, Black R, Topple A. Orientation of Listing's plane in normals and in patients with unilateral vestibular deafferentation. *Exp Brain Res*. 1994;101:525-528.
58. Suzuki Y, Kase M, Kato H, Fukushima K. Stability of ocular counterrolling and Listing's plane during static roll-tilts. *Invest Ophthalmol Vis Sci*. 1997;38:2103-2111.
59. Tweed D. Visual-motor optimization in binocular control. *Vis Res*. 1997;37:1939-1951.
60. Kapoula Z, Bernotas M, Haslwanter T. Listing's plane rotation with convergence: role of disparity, accommodation, and depth perception. *Exp Brain Res*. 1999;126:175-186.
61. Apt L. An anatomical reevaluation of rectus muscle insertions. *Trans Am Ophthalmol Soc*. 1980;78:365-375.
62. Bockisch CJ, Haslwanter T. Three-dimensional eye position during static roll and pitch in humans. *Vision Res*. 2001;41:2127-2137.
63. Thurtell MJ, Kunin M, Raphan T. Role of muscle pulleys in producing eye position-dependence in the angular vestibuloocular reflex: a model-based study. *J Neurophysiol*. 2000;84:639-650.